# CLAC Binds to Aggregated A$\beta$ and A$\beta$ Fragments, and Attenuates Fibril Elongation

Hiroyoshi Kakuyama,*,‡ Linda Söderberg,‡ Kazuhiko Horigome,§ Bengt Winblad,‡ Camilla Dahlqvist,‡ Jan Näslund,‡ and Lars O. Tjernberg‡

*Karolinska Institutet and Sumitomo Pharmaceuticals Alzheimer Center (KASPAC), Neurotec, Karolinska Institutet, SE-141 57 Huddinge, Sweden, and Research Division, Sumitomo Pharmaceuticals Company, Ltd., 3-1-98 Kasugade-naka, Konohana, Osaka 554-0022, Japan*

*Received July 1, 2005; Revised Manuscript Received September 26, 2005*

ABSTRACT: Deposition of amyloid $\beta$-peptide (A$\beta$) into amyloid plaques is one of the invariant neuropathological features of Alzheimer's disease. Proteins that codeposit with A$\beta$ are potentially important for the pathogenesis, and a recently discovered plaque-associated protein is the collagenous Alzheimer amyloid plaque component (CLAC). In this study, we investigated the molecular interactions between A$\beta$ aggregates and CLAC using surface plasmon resonance spectroscopy and a solid-phase binding immunoassay. We found that CLAC binds to A$\beta$ with high affinity, that the central region of A$\beta$ is necessary and sufficient for CLAC interaction, and that the aggregation state of A$\beta$ as well as the presence of negatively charged residues is important. We also show that this binding results in a reduced rate of fibril elongation. Taken together, we suggest that CLAC becomes involved at an intermediate stage in the pathogenesis by binding to A$\beta$ fibrils, including fibrils formed from peptides with truncated N- or C-termini, and thereby slows their growth.

Alzheimer's disease (AD)[1] is the most prevalent cause of dementia in elderly people. One of the defining neuropathological features of AD is the occurrence of senile plaques (SPs), which are mainly composed of fibrils formed from the 40−42-residue amyloid $\beta$-peptide (A$\beta$). A$\beta$ is derived from the $\beta$-amyloid precursor protein (APP), a type I transmembrane protein (*1*). The final step in A$\beta$ production is executed by the $\gamma$-secretase complex, critically dependent on presenilin 1 or 2 (*2*). The notion that polymerization of A$\beta$ into oligomers and larger species is particularly important for disease progression is supported by the identification of familial AD mutations in the APP and presenilin genes (*3*, *4*). Most of these mutations increase the production of the more fibrillogenic A$\beta$42 species, which is the initial A$\beta$ species to be deposited in SPs (*5*). Further evidence for the importance of A$\beta$ is AD-like pathology in Down's syndrome (DS) subjects, probably due to the extra copy of chromosome 21 containing the APP gene (*6*). Studies in transgenic mice and data from toxicity studies in cell culture also support the notion of the importance of A$\beta$ in AD (*7*). The mechanism whereby A$\beta$ monomers assemble into oligomers, larger aggregates, and finally into SPs is unclear. It is possible that the less dense A$\beta$ deposits, termed diffuse plaques, represent an early stage of A$\beta$ deposition. Support for this idea comes from studies in DS patients, where an age-dependent progression from diffuse plaques found in young DS subjects to the mature SPs found in adults is observed (*8*−*10*). In addition to A$\beta$, several other proteins such as glucosamine proteoglycans (*10*, *11*), complement factor C1q (*12*), apolipoprotein E (apoE) (*13*−*15*), and laminin (*16*) have been identified in the SPs. Many studies on these proteins suggest that they are able to modulate A$\beta$ aggregation (*16*, *17*). It is likely that other, yet uncharacterized, proteins also affect the aggregation process.

One newly discovered plaque-associated protein, collagenous Alzheimer amyloid plaque component (CLAC), was identified in a screen using monoclonal antibodies raised against crude amyloid preparations isolated from human AD brain (*18*). Recently, we showed that the previously reported plaque-associated protein AMY (*19*, *20*) was identical to CLAC (*21*). CLAC is expressed in neurons and belongs to the collagenous transmembrane group of proteins which currently consists of eight members (*22*). CLAC is generated through furin cleavage of the type II transmembrane protein CLAC-P (collagen type XXV) (*18*). CLAC is copurified with amyloid-enriched fractions from human AD brain (*18*, *21*) and shows extensive colocalization with SPs in AD and DS brains, whereas no CLAC immunoreactivity has been shown in cerebrovascular amyloid (*18*, *21*). Despite some immunohistochemical observations (*18*, *21*, *23*) it is still poorly understood how CLAC contributes to the pathogenesis of AD. A recent in vitro study suggests an inhibitory role of CLAC on A$\beta$ fibril formation (*24*), while we show an

* To whom correspondence should be addressed: Karolinska Institutet, Neurotec, Novum, KASPAC pl. 5, SE-141 57 Huddinge, Sweden. Telephone: +46 8 585 836 25. Fax: +46 8 585 836 10. E-mail: hiroyoshi.kakuyama@neurotec.ki.se.

‡ Novum.

§ Sumitomo Pharmaceuticals Co., Ltd.

[1] Abbreviations: AD, Alzheimer's disease; apoE, apolipoprotein E; APP, amyloid precursor protein; A$\beta$, amyloid $\beta$-peptide; EDC, *N*-ethyl-*N*′-[3-(dimethylamino)propyl]carbodiimide; HBS-EP, 10 mM HEPES (pH 7.4), 150 mM NaCl, 3 mM EDTA, and 0.005% Tween 20; NHS, *N*-hydroxysuccinimide; PBS, phosphate-buffered saline; RU, resonance unit; SPR, surface plasmon resonance; SPs, senile plaques; ThT, thioflavin T.

10.1021/bi051263e CCC: $30.25 © 2005 American Chemical Society
Published on Web 11/03/2005

assembly of Aβ fibrils into large and more protease resistance aggregates in the presence of CLAC (*25*). Thus, it is possible that CLAC has a dual role in AD pathogenesis.

Surface plasmon resonance (SPR) spectroscopy is a widely used technique for studies of molecular interactions, and has been used to analyze Aβ−Aβ binding (*26*). Here we use SPR spectroscopy and a solid-phase binding immunoassay to study interactions between CLAC and Aβ. Previously, we identified an eight-amino acid sequence in CLAC that is crucial for Aβ binding (*27*), and here we search for determinants in Aβ that mediate CLAC binding. We show that CLAC binds to aggregated but not to nonaggregated Aβ and central fragments thereof (Aβ10−20 and Aβ12−28), and that this binding is partly dependent on ionic interactions. In addition, we show by SPR spectroscopy that CLAC reduces the rate of Aβ fibril elongation. Collectively, these data suggest that CLAC binds to Aβ fibrils, including fibrils formed from Aβ peptides with truncated N- and/or C-termini, resulting in a decrease in the rate of fibril Aβ elongation.

## EXPERIMENTAL PROCEDURES

*Samples and Reagents.* The recombinant CLAC used in this study was cloned from a human brain cDNA library (*21*), expressed and purified as described previously (*27*). Biotinylated Aβ1−40 and Aβ1−42 were purchased from rPeptide (Athens, GA). Aβ10−20 was purchased from American Peptide Company Inc. (Sunnyvale, CA), and the Aβ10−20 mutants YAVHHQKLVFF (Aβ10−$20^{A11}$), YEVAA-QKLVFF (Aβ10−$20^{AA13,14}$), and YEVHHQKLVAA (Aβ10−$20^{AA19,20}$) were from Invitrogen Corp. (Carlsbad, CA). All other peptides were purchased from Bachem AG (Bubendorf, Switzerland). Human laminin, apoE, and bovine serum albumin (BSA) were purchased from Chemicon International Inc. (Temecula, CA) and Sigma (St. Louis, MO). The anti-myc antibody was from Invitrogen. The sensor chips used were research-grade CM5, CM3, and streptavidin (SA)-coated sensor chips (Biacore AB, Uppsala, Sweden). The coupling reagents *N*-ethyl-*N*′-[3-(dimethylamino)propyl]carbodiimide (EDC), *N*-hydroxysuccinimide (NHS), and ethanolamine were purchased from Biacore AB.

*Surface Plasmon Resonance Spectroscopy*. Surface plasmon resonance (SPR) spectroscopy analysis was performed on a BIAcore 3000 instrument (Biacore AB). Biotinylated and nonbiotinylated Aβ peptides were mixed (1:10) with ultrapure water to a peptide concentration of 200 μM. This solution was stirred for 5 min before addition of 2× phosphate-buffered saline (PBS, pH 7.4) to a final Aβ concentration of 100 μM and stirred for an additional 2 days. Fibrils were sedimented by centrifugation at 10000*g* for 10 min, and the supernatant was replaced with an equal volume of HBS-EP [10 mM HEPES (pH 7.4), 150 mM NaCl, 3 mM EDTA, and 0.005% Tween 20 (Biacore AB)]. A thioflavin T (ThT)-based assay (see below) was used to confirm that the samples were aggregated. Aggregates were aliquoted and stored at −70 °C until they were used. SA chips were used to capture biotinylated nonaggregated or aggregated Aβ1−40. The increase in response units, reflecting the amount of immobilized material, was recorded. One hundred microliters of CLAC in running buffer (1.56−25 nM) was injected at a flow rate of 40 μL/min (association phase). After injection, the sensor chip was washed with running buffer for 600 s (dissociation phase). The assays were performed at 25 °C, and the surface of the flow cells was regenerated by injection of 100 mM citrate buffer (pH 4.0). The response from a nonderivatized flow cell was subtracted to compensate for nonspecific binding. Different concentrations of laminin (12.5, 25, and 50 nM), apoE (90, 180, and 360 nM), and BSA (3.1 μM) in HBS-EP were injected over an SA chip coated with aggregated Aβ1−40 (795 RU) and analyzed as described above.

Table 1: Binding Affinity of CLAC for Aggregated Aβ Fragments Analyzed by SPR Spectroscopy[a]

| | Aβ1−42 | Aβ1−40 | Aβ1−28 | Aβ12−28 |
|---|---|---|---|---|
| $k_a$ ($\times 10^{-5}$ $M^{-1}$ $s^{-1}$) | 2.9 ± 0.3 | 3.8 ± 1.5 | 6.1 ± 0.9 | 6.0 ± 1.3 |
| $k_d$ ($\times 10^4$ $s^{-1}$) | 4.0 ± 0.1 | 2.7 ± 0.8 | 5.2 ± 1.0 | 11.1 ± 4.5 |
| $K_d$ (nM) | 1.4 ± 0.4 | 0.9 ± 0.5 | 0.9 ± 0.3 | 2.0 ± 1.1 |
| $\chi^2$ | 0.73 ± 0.59 | 1.01 ± 1.04 | 1.79 ± 1.41 | 0.81 ± 0.60 |

[a] Aggregated Aβ fragments were immobilized on CM5 sensor chips. CLAC was injected at different concentrations (1.56−25 nM). The kinetic rate constants were analyzed using simultanous fitting of $k_a$ and $k_d$ in a Langmuir 1:1 model (A + B ↔ AB), and the parameters are means ± standard deviation.

Table 2: Protocol for Measurement of Aβ Elongation

| cycle no. | step 1 (pretreatment) | step 2 (Aβ elongation) | step 3 (regeneration) |
|---|---|---|---|
| 1 | PBS | | |
| 2 | 100 nM CLAC | | |
| 3 | PBS | | |
| 4 | 50 nM CLAC | | |
| 5 | PBS | | |
| 6 | 100 nM CLAC | 15 μM | 100 nM |
| 7 | PBS | Aβ1−40 | citrate twice |
| 8 | 50 nM CLAC | | |
| 9 | PBS | | |
| 10 | 100 nM CLAC | | |
| 11 | PBS | | |
| 12 | 50 nM CLAC | | |

*SPR Analysis of the CLAC Binding Site in Aβ*. Aβ-related peptides were aggregated for 10 days at various concentrations: 100 μM for Aβ1−40, 50 μM for Aβ1−42 and Aβ29−40, and 200 μM for Aβ1−28 and Aβ12−28. Aggregated material was collected as described above and resuspended in HBS-EP to a concentration of 10 μM, further diluted to 0.5 μM in 10 mM sodium acetate buffer (pH 4.0), and sonicated on ice with a microprobe. CM5 chips were used to immobilize the aggregated peptides by standard amine coupling chemistry. CLAC binding was studied as described above.

*Data Processing and Kinetics*. The sensorgrams for CLAC (1.56−25 nM) were fitted globally to a Langmuir 1:1 binding model (A + B ↔ AB) using BIAevaluation version 4.0.1.

*SPR Analysis of Aβ Fibril Elongation.* Aβ was aggregated in PBS for 24 h at a concentration of 100 μM, diluted to 10 μM in PBS, and further diluted to 0.5 μM in 10 mM sodium acetate buffer (pH 4.0) before being immobilized to a CM3 chip by standard amine coupling chemistry. In total, 12 cycles were performed in a sequential order with CLAC present in every even-numbered cycle (Table 2). Each cycle was made up of three steps: treatment with CLAC or PBS, Aβ association, and regeneration. In the first step, PBS or CLAC

(50 or 100 nM) was injected at a flow rate of 5.0 $\mu$L/min for 6 min. In the second step, A$\beta$ (15 $\mu$M) was injected at a flow rate of 30 $\mu$L/min for 1 min. After one cycle, the sensor chip was regenerated with 100 mM citrate buffer (two injections, 1 min each) to remove CLAC from the A$\beta$ fibrils as the third step.

*Calculation of Elongation Kinetics.* Data were analyzed using BIAevaluation version 4.0.1. The elongation rate was calculated as the difference in response units at the end and the beginning of the injection of A$\beta$. The CLAC dissociation rate was compensated for using formula 1: A$\beta$ elongation rate = slope of A$\beta$ elongation phase − slope of CLAC dissociation phase. The sensorgrams from odd-numbered cycles (without CLAC) were used to calculate the elongation rate in the absence of CLAC, and the same analysis was performed for even-numbered cycles (with CLAC). We compared the elongation rates in the presence and absence of CLAC. A power curve was fitted to the obtained values from each injection in the absence of CLAC. The formula describing the curve was used to calculate the elongation rate in the absence of CLAC, and the even-numbered cycle's elongation rate was estimated. The ratio of elongation rates was calculated by dividing the measured elongation rate in the presence of CLAC by the estimated elongation rate in the absence of CLAC from the power curve. Significance was determined by a two-tailed Dunnett's multicomparison test. Significance was reported at the 95% ($p < 0.05$) confidence level.

*Solid-Phase Binding Immunoassay.* A solid-phase binding immunoassay described previously (*28*) was used with minor modifications. Briefly, peptides were dissolved in dimethyl sulfoxide (DMSO, 99.9%, Sigma) and diluted in PBS to 20 or 2.0 $\mu$M. Fifty microliters of A$\beta$ peptide solution (1.0 or 0.1 nmol/well) was allowed to dry and bind overnight at 37 °C in microtiter wells (MaxiSorp, Nunc A/S, Roskilde, Denmark). Blocking was performed with 300 $\mu$L of PBS containing 0.4% blocking reagent (Roche Diagnostics GmbH, Mannheim, Germany) for 1 h followed by washing with PBS containing 0.05% Tween 20 (PBS-T) in a microplate washer (ASYS Hitech, Atlantis, GmbH, Eugendolf, Austria). Conditioned medium from cells stably expressing CLAC was diluted in PBS containing NP40 (IGEPAL CA-630, Sigma) (final concentration of 0.005%), and 50 $\mu$L was applied to the wells coated with different A$\beta$ peptides and incubated for 1 h at room temperature. The wells were washed with PBS-T and incubated with anti-myc antibody (1:5000 in blocking buffer) for 1 h. The procedure was repeated for the anti-mouse secondary antibody conjugated to horseradish peroxidase (Amersham Biosciences, 1:6000 dilution). The wells were rinsed with PBS-T, and 100 $\mu$L of peroxidase substrate solution (ImmunoPure TMB substrate kit, Pierce, Rockford, IL) was added. The reaction was stopped with 100 $\mu$L of 2 M $H_2SO_4$, and absorbance was measured at 450 nm in a microplate reader (FLUOstar Galaxy, BMG Labtechnologies GmbH, Offenburg, Germany).

*Thioflavin T Binding Assay.* To measure the amount of aggregated peptide bound to the mictrotiter plate wells, we used a ThT binding assay. One-hundred ninety microliters of ThT [5 $\mu$M in 50 mM glycine-NaOH buffer (pH 8.5)] was added to each well, and the fluorescence was measured (excitation at 440 nm and emission at 490 nm) in a microplate reader (FLUOstar Galaxy).

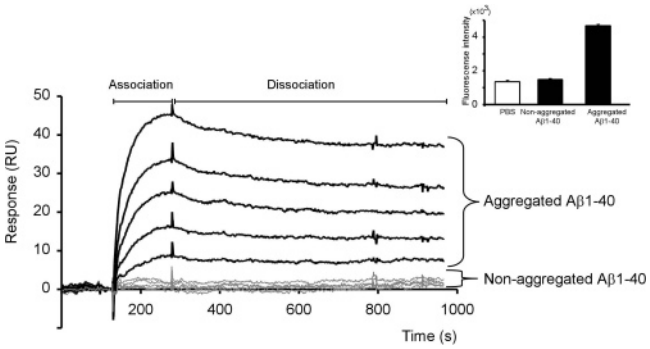


FIGURE 1: CLAC binds to aggregated A$\beta$. Binding of CLAC to aggregated and nonaggregated A$\beta$ was studied using SPR spectroscopy. Nonaggregated biotin-bound A$\beta$1−40 (85 RU) or aggregated A$\beta$1−40 (biotin-bound A$\beta$1−40:A$\beta$1−40 ratio of 1:10) (76 RU) was immobilized onto a streptavidin (SA) sensor chip. CLAC in HBS-EP was injected at different concentrations (from 1.56 to 25 nM) at 25 °C at a flow rate of 40 $\mu$L/min, and the binding curves from control surfaces (no peptide immobilized) were subtracted. The bars indicate the association phase and the dissociation phase. The inset shows the ThT response for biotin-bound A$\beta$1−40 and for aggregated biotin-bound A$\beta$1−40.

## RESULTS

*CLAC Binds to Aggregated A$\beta$.* CLAC was recently found to bind to aggregated A$\beta$ (*18*). Here, we use SPR spectroscopy to study this interaction in more detail. The advantage of this technique is that the binding is studied in real time and no additional steps (such as centrifugation) or reagents (such as ThT) are needed. Freshly solubilized biotinylated A$\beta$1−40 was immobilized to streptavidin (SA) sensor chips in separate flow cells (designated nonaggregated A$\beta$1−40). Biotinylated and nonbiotinylated A$\beta$1−40 (1:10) were mixed, allowed to aggregate, and immobilized in a separate flow cell (designated aggregated A$\beta$1−40). The amounts of immobilized aggregated A$\beta$1−40 (76 RU) and nonaggregated A$\beta$1−40 (85 RU) were similar. Different concentrations of CLAC (1.56−25 nM) were injected (Figure 1). The first part of these curves represents running buffer flowing past the sensor surface, the ascending part of the curve corresponds to the binding of CLAC to immobilized A$\beta$, and the descending part corresponds to the dissociation of CLAC after termination of the injection (only running buffer flows past the sensor surface). CLAC bound to aggregated A$\beta$, while no interaction was observed with nonaggregated species (Figure 1). A ThT-based assay was used to verify the aggregation state of the samples (inset of Figure 1). For the kinetic analysis of binding of CLAC to aggregated A$\beta$, different amounts of aggregated A$\beta$ were immobilized (76, 332, and 795 RU) and CLAC (1.56−25 nM) was injected. The sensorgrams were analyzed using global fitting to the Langmuir 1:1 binding model (A + B $\leftrightarrow$ AB). The model was chosen on the basis of the residual plots, the values of $\chi^2$, and visual inspection of the fitted curves. The rate constants and the affinity were calculated: $k_a = (6.5 \pm 0.4) \times 10^{-5}$ M$^{-1}$ s$^{-1}$, $k_d = (3.7 \pm 0.8) \times 10^4$ s$^{-1}$, and $K_d = 0.6 \pm 0.1$ nM ($\chi^2 = 10.3 \pm 6.1$).

To compare the affinity of CLAC for A$\beta$ with the affinity of other proteins for A$\beta$, we studied the well-characterized plaque-associated proteins laminin and apoE. Laminin (50 nM) or apoE (360 nM) was injected over a SA chip with immobilized A$\beta$ (Figure 2). The affinity was found to be $2.6 \pm 0.6$ nM for laminin and $6.0 \pm 2.7$ nM for apoE. Thus,

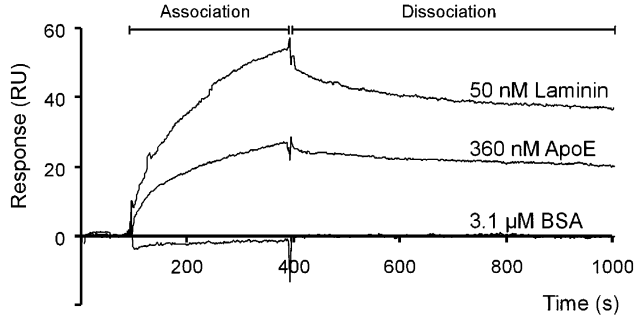


FIGURE 2: Binding of laminin, apoE, and BSA to aggregated Aβ1−40. Aggregated Aβ1−40 (biotinylated Aβ1−40:Aβ1−40 ratio of 1:10, 795 RU) was immobilized onto a streptavidin (SA) sensor chip. Laminin (50 nM), apoE (360 nM), or BSA (3.1 μM) in HBS-EP buffer was injected at 25 °C at a flow rate of 10 μL/min. Binding curves from control surfaces (no peptide immobilized) were subtracted. The bars indicate the association phase and the dissociation phase.

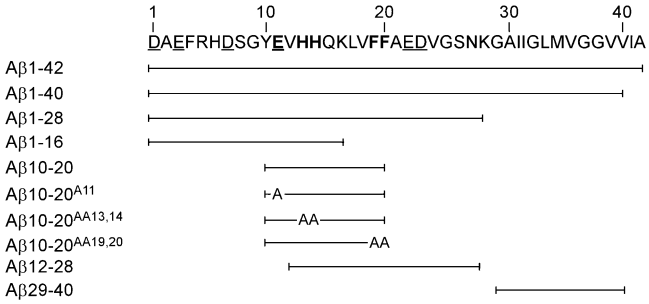


FIGURE 3: Schematic picture of Aβ1−42 and shorter Aβ sequences used in SPR spectroscopy and the solid-phase binding immunoassay. The primary sequence of Aβ1−42 is given in one-letter code. The negatively charged residues are underlined, and residues in bold are substituted in some of the fragments used.

CLAC appears to have a relatively high affinity for aggregated Aβ. The negative control BSA did not bind to Aβ (Figure 2).

*The Central Region of Aβ Is Necessary and Sufficient for CLAC Binding.* We investigated by SPR spectroscopy and with a solid-phase binding immunoassay whether a specific CLAC binding region exists in Aβ. Aggregates formed from Aβ1−42 or shorter Aβ sequences were immobilized on CM5 sensor chips (Figure 3). CLAC showed strong binding to Aβ1−42, Aβ1−40, and Aβ1−28, intermediate binding to Aβ12−28, and considerably weaker binding to the C-terminal fragment Aβ29−40 (even when the amount of immobilized peptide was more than 4000 RU) (Figure 4A−D and Table 1). To investigate whether electrostatic interactions were involved in the binding of CLAC to Aβ, we varied the concentration of sodium chloride in the washing buffer. An increased concentration had the same effect on Aβ1−28, Aβ12−28, Aβ1−40, and Aβ1−42, abolishing the interaction at a concentration of ∼0.5 M (data not shown). We conclude that the C-terminal part of Aβ is dispensable, and that the binding is partly dependent on ionic interactions.

We further evaluated the avidity of CLAC for the peptides by a different assay. The Aβ peptides, Aβ1−42, Aβ1−40, Aβ1−28, Aβ1−16, Aβ12−28, Aβ10−20, and Aβ29−40, were allowed to aggregate, coated onto microtiter plate wells, and incubated with conditioned media containing CLAC. Under these conditions, CLAC bound to Aβ1−40 and Aβ1−28 to a similar extent (100 and 85%, respectively) as to Aβ1−42 (set to 100%) (Figure 5A). CLAC bound to Aβ10−20 and Aβ12−28 with intermediate avidity (44 and 20%, respectively), while the avidity for Aβ1−16 and Aβ29−40 was weak (Figure 5A). The amount of immobilized peptide aggregates was measured by ThT fluorescence (Figure 5B). Aβ1−42 exhibited the highest fluorescence intensity, and this value was set to 100%. Aβ1−40 exhibited an intensity of 40%, Aβ1−28 30%, Aβ29−40 20%, and Aβ10−20 as well as Aβ12−28 10%. The Aβ1−16 fluorescence was close to background levels, indicating that no aggregates had formed (we do not exclude the possibility that aggregates formed by this negatively charged fragment could bind

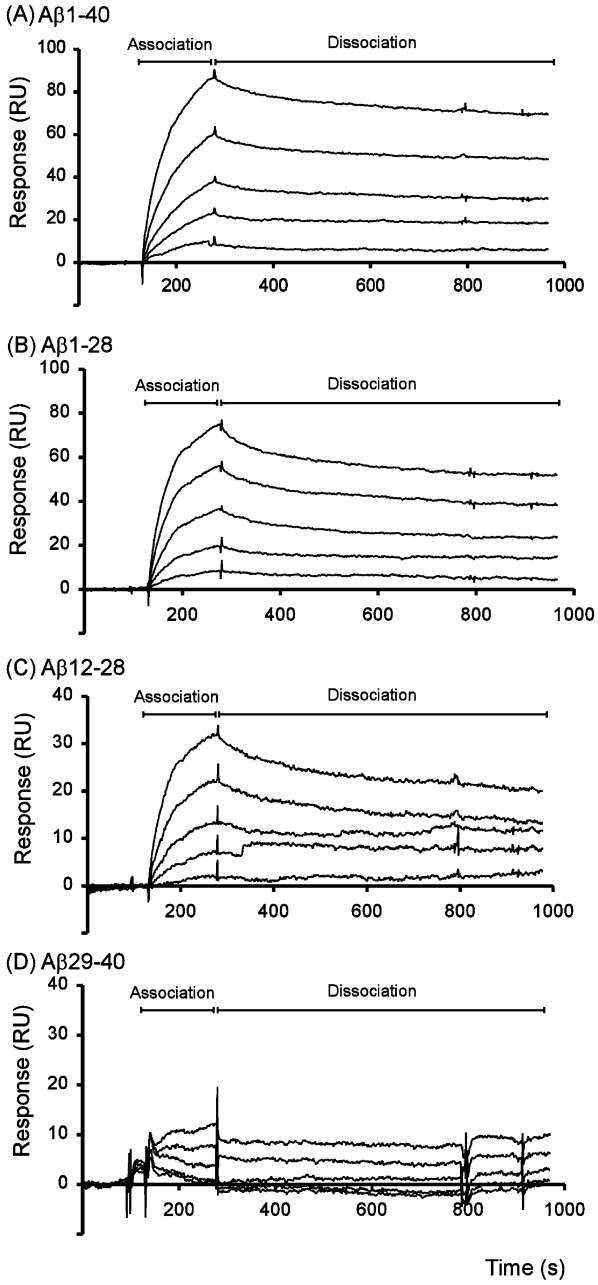


FIGURE 4: Interaction of CLAC with various aggregated Aβ fragments. Aggregated Aβ species (A) Aβ1−40 (1080 RU), (B) Aβ1−28 (549 RU), (C) Aβ12−28 (730 RU), and (D) Aβ29−40 (4170 RU) were immobilized onto a CM5 chip using standard amine coupling chemistry. CLAC in HBS-EP was injected at different concentrations (1.56−25 nM) at 25 °C at a flow rate of 40 μL/min. Binding curves from control surfaces (no peptide immobilized) were subtracted. The bars indicate the association phase and the dissociation phase.

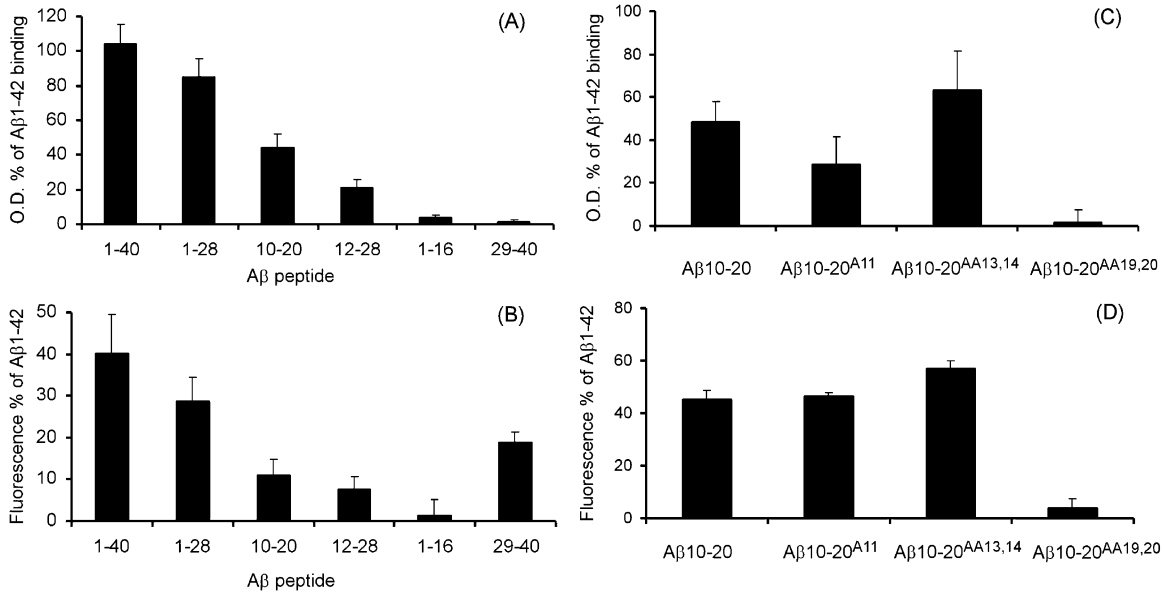


FIGURE 5: CLAC binds to aggregated, charged A$\beta$ species. CLAC−A$\beta$ solid-phase binding immunoassay. (A) Conditioned medium from HEK293 cells stably expressing CLAC was incubated with different A$\beta$ fragments immobilized in microtiter wells (0.1 nmol/well). Percentages of A$\beta$1−42 binding are shown. The bars represent the mean ± the standard deviation ($n$ = 3). (B) ThT fluorescence of immobilized A$\beta$ fragments. Aggregated A$\beta$ fragments immobilized in microtiter wells (0.1 nmol/well) were incubated with ThT (5 $\mu$M), and fluorescence was recorded. The fluorescence from the A$\beta$1−42 sample was set to 100%. The bars represent the mean ± the standard deviation ($n$ = 3). (C) A$\beta$10−20 and its mutant analogues A$\beta$10−20$^{A11}$, A$\beta$10−20$^{AA13,14}$, and A$\beta$10−20$^{AA19,20}$ were allowed to aggregate and were immobilized in microtiter wells (1.0 nmol/well). Conditioned medium from HEK293 cells stably expressing CLAC was incubated with different A$\beta$ fragments immobilized in microtiter wells (0.1 nmol/well). Presented are percentages of A$\beta$1−42 binding. The bars represent the mean ± the standard deviation ($n$ = 3). (D) ThT fluorescence of immobilized A$\beta$10−20 and its mutant analogues. A$\beta$ fragments immobilized in microtiter wells (1.0 nmol/well) were incubated with ThT (5 $\mu$M), and fluorescence was recorded. Presented are percentages of the fluorescence from the 0.1 nmol A$\beta$1−42 well. The bars represent the mean ± the standard deviation ($n$ = 3).

CLAC). If the amount of immobilized aggregated peptide is taken into account, A$\beta$12−28 and A$\beta$10−20 could be considered strong CLAC binders. Hence, both aggregated A$\beta$12−28 and A$\beta$10−20 contain sufficient information for CLAC binding.

The shortest fragment required for efficient CLAC binding was the A$\beta$10−20 peptide. To investigate the importance of charged residues, we studied two mutant A$\beta$10−20 peptides (Figure 3). In one of these, the His residues at positions 13 and 14 were exchanged for Ala (A$\beta$10−20$^{AA13,14}$), resulting in a less positively charged peptide, and in the other, the Glu residue in position 11 was exchanged for Ala (A$\beta$10−20$^{A11}$), resulting in a less negatively charged peptide. In a third peptide, the Phe residues at positions 19 and 20 were substituted with Ala (A$\beta$10−20$^{AA19,20}$) (Figure 3). We chose Phe-19 and Phe-20 since they are critical for A$\beta$ fibril formation (*29*−*31*). Neither CLAC binding nor ThT response was affected by the His to Ala substitutions (Figure 5C,D). A$\beta$10−20$^{A11}$ exhibited only half of the CLAC binding as compared to wild type, while the amount of fibrils was intact as indicated by the ThT response. In the case of the A$\beta$10−20$^{AA19,20}$ mutant, both CLAC binding and ThT fluorescence were abolished. HPLC analysis showed that similar amounts of the mutants were immobilized in the wells (data not shown), indicating that the lack of A$\beta$10−20$^{AA19,20}$ aggregates (as determined by ThT) accounts for the loss of CLAC binding.

*CLAC Reduces the Rate of Elongation of A$\beta$ Fibrils.* To investigate the effect of binding of CLAC to A$\beta$ fibrils, we developed a procedure for studying A$\beta$ fibril elongation in the presence of CLAC. Previous reports have demonstrated that SPR spectroscopy is a useful method for analysis of

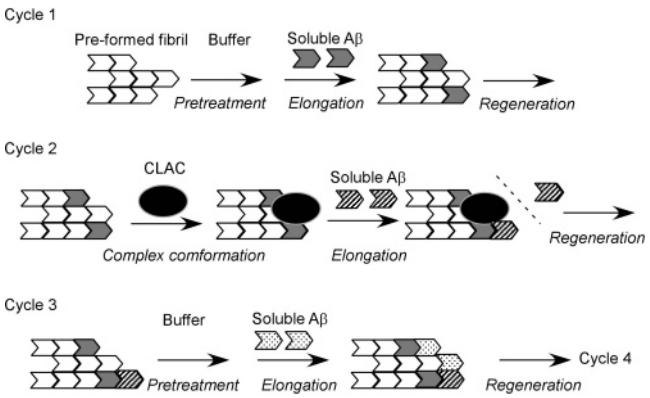


FIGURE 6: Procedure for A$\beta$ fibril elongation. Aggregated A$\beta$1−40 was immobilized on the sensor chip (CM3) using standard amine coupling chemistry. In the odd-numbered cycles, buffer was injected over the surface followed by injection of soluble A$\beta$1−40 (15 $\mu$M) (elongation step), whereafter the chip was washed with 100 mM citrate to remove unspecifically bound A$\beta$. In the even-numbered cycles, CLAC was injected over fibrils followed by injection of soluble A$\beta$1−40 (15 $\mu$M) (elongation step), whereafter the chip was washed with 100 mM citrate to remove unspecifically bound A$\beta$.

A$\beta$ fibril elongation (*32*, *33*), and we refined this approach (Figure 6 and Table 2). First, we immobilized A$\beta$ fibrils and measured the fibril elongation rate by injecting a solution of freshly dissolved A$\beta$ (1.89−30 $\mu$M). The rate of elongation was concentration-dependent (Figure 7A), and the elongation rate was reproducible for several cycles of elongation and washing. Next, we examined the effect of CLAC on A$\beta$ fibril elongation (Figure 7B,C) according to the protocol in Table 2 and Figure 6. The rate of fibril elongation in the presence and absence of CLAC was

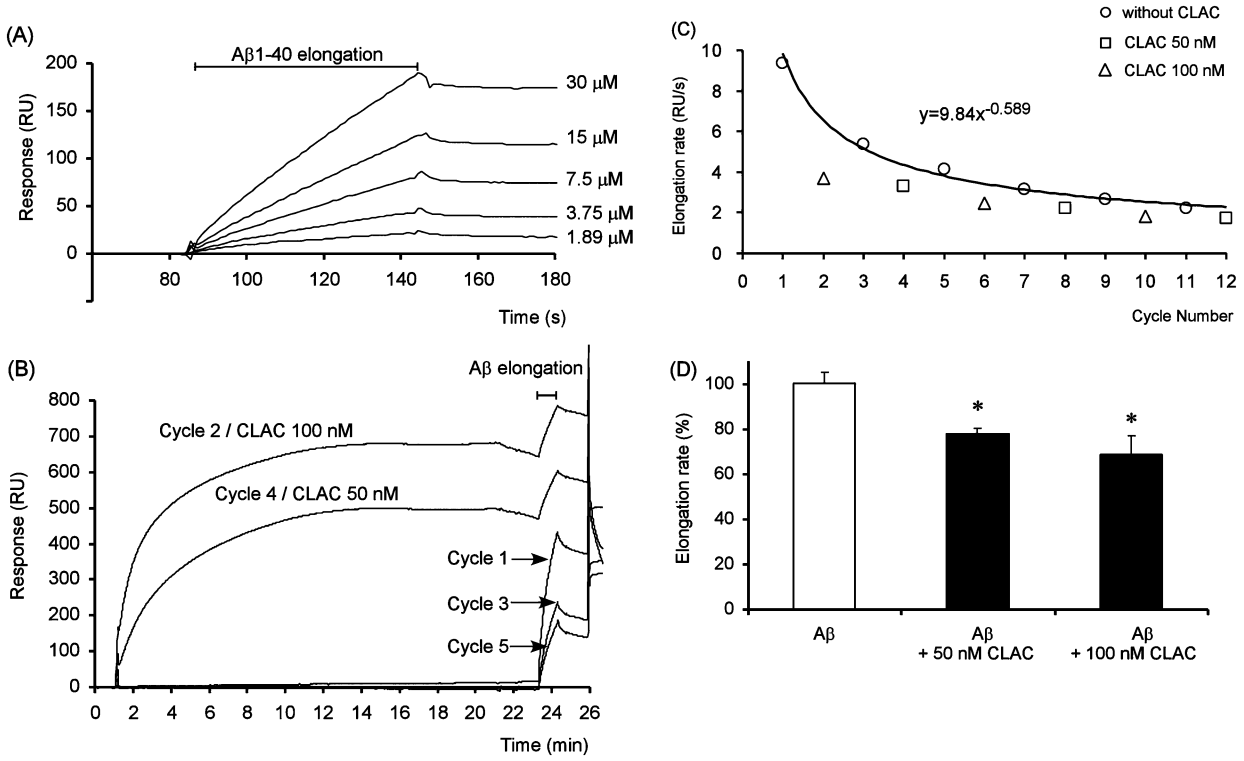


FIGURE 7: Characterization of A$\beta$ fibril elongation. (A) Different concentrations of freshly dissolved A$\beta$1−40 were injected over immobilized aggregated A$\beta$1−40 (2120 RU) at a flow rate of 30 $\mu$L/min for 1 min. (B) A typical sensorgram showing the elongation of A$\beta$1−40 fibrils in the presence or absence of CLAC. Aggregated A$\beta$1−40 was immobilized on a CM3 chip (1580 RU). CLAC (50 or 100 nM) or PBS was injected, and the elongation rate was calculated according to formula 1. (C) A power curve was fitted to the A$\beta$1−40 fibril elongation rates obtained in the absence of CLAC (odd-numbered cycles). The elongation rates in the presence of CLAC are plotted as squares (50 nM CLAC) and triangles (100 nM CLAC). (D) The ratio of the fibril elongation rate in the presence of CLAC and the corresponding value in the absence of CLAC, as obtained from the power curve, were calculated. The statistical analysis was by a two-tailed Dunnett multicomparison test. Significance vs the elongation rate in the absence of CLAC was reported at the 95% level ($p < 0.05$). The result represent the mean ± the standard deviation from two different flow cells.

Table 3: A$\beta$ Elongation Rates

| [CLAC] (nM) | cycle no. | calculated in the absence of CLAC | observed in the presence of CLAC | ratio (%) |
|---|---|---|---|---|
| 50 | 4 | 4.3 | 3.3 | 76 |
| | 8 | 2.9 | 2.2 | 78 |
| | 12 | 2.3 | 1.7 | 76 |
| 100 | 2 | 6.5 | 3.7 | 57 |
| | 6 | 3.4 | 2.5 | 72 |
| | 10 | 2.5 | 1.8 | 72 |

calculated according to formula 1 (see Experimental Procedures). A curve was fitted to the observed elongation rates in the absence of CLAC according to the relation $y = bx^c$, where $b = 9.85$ and $c = -0.894$ ($r^2 = 0.988$). The rate of A$\beta$ fibril elongation was higher in the absence of CLAC (Figure 7C). The rates obtained in the presence of CLAC were divided by the rates in the absence of CLAC as obtained from the power curve (Table 3). Treatment with 50 and 100 nM CLAC reduced the rate of fibril elongation to 78 and 69%, respectively (Figure 7D). Hence, CLAC binds to A$\beta$ fibrils and attenuates their elongation.

## DISCUSSION

The interaction between A$\beta$ and plaque-associated proteins such as apoE, glucosamine proteoglycans, and α1-antichymotrypsin appears to be important for the pathogenesis of AD. It is also possible that the newly discovered plaque-associated protein CLAC has a role in AD. Recent in vitro studies indicate that positively charged motifs in CLAC and the aggregation state of A$\beta$ are important for CLAC−A$\beta$ interaction (*24*, *27*). In this study, we use SPR spectroscopy and a solid-phase binding immunoassay to show that (i) CLAC binds to aggregated A$\beta$ with high affinity, (ii) the central region of A$\beta$ (A$\beta$10−20 or A$\beta$12−28) is sufficient and necessary for CLAC binding, (iii) the binding is partly mediated by negatively charged residues in A$\beta$, and (iv) CLAC attenuates the rate of A$\beta$ fibril elongation.

*CLAC Binds to* A$\beta$ *Aggregates.* Previous studies on CLAC−A$\beta$ interactions have only provided a single point measurement of binding affinity, with no information about the kinetics of binding. In this study, we use SPR spectroscopy to further investigate the interaction between A$\beta$ and CLAC. We find that CLAC binds to aggregated A$\beta$ in a concentration-dependent manner (Figure 1), with an apparent $K_d$ of ∼0.6 nM. This affinity is ∼10 times higher than apoE's affinity for A$\beta$ as determined by SPR spectroscopy (6−10 nM, Figure 2 and ref *34*).

*Is There a Specific CLAC Binding Sequence in A$\beta$?* We have identified a sequence (LIKRRLIK) in the non-collagen domain 2 of CLAC that is crucial for binding to A$\beta$ (*27*), and other positively charged CLAC sequences could be important for A$\beta$ binding (*24*). Since the binding involves ionic interactions, it is reasonable to speculate that the positively charged CLAC motif binds to the negatively charged N-terminal part of A$\beta$, and a recent report suggested the CLAC binding domain of A$\beta$ is located in A$\beta$1−16 (*24*). We show that CLAC binds to aggregates formed from

peptides containing residues 12−20 of A$\beta$ (e.g., A$\beta$12−28 or A$\beta$10−20), but not to aggregated A$\beta$29−40. Since A$\beta$29−40 (in contrast to the CLAC binding peptides) does not contain any charged residues, it appears that, in addition to the quaternary structure of A$\beta$, charged residues are important for CLAC binding. Now, since the N-terminal and C-terminal parts of A$\beta$ (residues 29−40 and 1−9, respectively) seem to be optional for CLAC binding, we focus on residues 10−28. This sequence contains the following residues (one-letter code and negative residues underlined): YEVHHQKLVFFAEDVGSNK. Note that this sequence harbors three negatively charged residues, but none of these are shared between A$\beta$10−20 and A$\beta$12−28. The positively charged histidines can be replaced with alanines without any significant effect on CLAC binding, suggesting that the sequence specificity is low. On the other hand, replacing Glu with Ala results in a peptide with reduced avidity for CLAC. The A$\beta$ sequence of residues 16−20 is the core A$\beta$ fibril forming motif (*29*−*31*), and substitution of Phe-19 with proline impairs fibril growth (*35*). In our study, substitution of residues Phe-19 and Phe-20 in A$\beta$10−20 inhibited aggregation and abolished CLAC binding, again showing that A$\beta$ fibril formation is imperative for this interaction (Figure 5C,D). We speculate that CLAC is a promiscuous binder of aggregates formed from peptides containing negatively charged residues.

*A Role for CLAC in Aβ Fibril Deposition.* We show by a further developed SPR spectroscopy procedure that treatment of A$\beta$ fibrils with CLAC decreases the rate of A$\beta$ fibril elongation by 20−30%. Previous results of Osada et al. (*24*) using the fibril labeling dye ThT suggest that CLAC inhibits fibril elongation by 75%. The discrepancy may be explained by differences in CLAC concentrations (Osada used higher concentrations), or masking effects in the ThT binding assay (*25*). A model explaining the inhibition of fibril elongation could be one in which CLAC binds to the ends of the emerging fibrils, thereby decreasing the rate of elongation. This model does not exclude the possibility that CLAC binds to other parts of the fibril. It is possible that CLAC could reduce fibril growth also in vivo. Interestingly, recent data suggest that the addition of A$\beta$ monomers to the fibril ends is crucial for A$\beta$-mediated toxicity (*36*). Thus, CLAC may suppress this interaction and have a protective role in AD. An additional effect of CLAC is that it assembles A$\beta$ fibrils into larger aggregates (*25*), and this might occur also in vivo. Studies in transgenic mice with altered CLAC expression will improve our understanding of CLAC's role in Alzheimer's disease.

## ACKNOWLEDGMENT

We thank Youich Oohba and Jiro Akimaru for the purification of CLAC. We also thank Shinichi Kojima and Akira Ito for meaningful discussions.

## REFERENCES

1. Hardy, J., and Selkoe, D. J. (2002) The amyloid hypothesis of Alzheimer's Disease: Progress and problems on the road to therapeutics, *Science 297*, 353−356.
2. Sisodia, S. S., and St George-Hyslop, P. H. (2002) $\gamma$-Secretase, notch, A$\beta$ and Alzheimer's disease: Where do the presenilins fit in? *Nat. Rev. Neurosci. 3*, 281−290.
3. Selkoe, D. J. (2002) Deciphering the genesis and fate of amyloid $\beta$-protein yields novel therapies for Alzheimer disease, *J. Clin. Invest. 110*, 1375−1381.
4. St George-Hyslop, P. H. (2000) Molecular genetics of Alzheimer's disease, *Biol. Psychol. 47*, 183−199.
5. Hardy, J. (1997) Amyloid, the presenilins and Alzheimer's disease, *Trends Neurosci. 20*, 154−159.
6. Barbiero, L., Benussi, L., Ghidoni, R., Alberici, A., Russo, C., Schettini, G., Pagano, S. F., Parati, E. A., Mazzoli, F., Nicosia, F., Signorini, S., Feudatari, E., and Binetti, G. (2003) BACE-2 is overexpressed in Down's syndrome, *Exp. Neurol. 182*, 335−345.
7. Gotz, J., Schild, A., Hoerndli, F., and Pennanen, L. (2004) Amyloid-induced neurofibrillary tangle formation in Alzheimer's disease: Insight from transgenic mouse and tissue-culture models, *Int. J. Dev. Neurosci. 22*, 453−465.
8. Stoltzner, S. E., Grenfell, T. J., Mori, C., Wisniewski, K. E., Wisniewski, T. M., Selkoe, D. J., and Lemere, C. A. (2000) Temporal accrual of complement proteins in amyloid plaques in Down's syndrome with Alzheimer's disease, *Am. J. Pathol. 156*, 489−499.
9. Mann, D. M. (1989) Cerebral amyloidosis, ageing and Alzheimer's disease: A contribution from studies on Down's syndrome, *Neurobiol. Aging 10*, 397−399.
10. Castillo, G. M., Ngo, C., Cummings, J., Wight, T. N., and Snow, A. D. (1997) Perlecan binds to the $\beta$-amyloid proteins (A$\beta$) of Alzheimer's disease, accelerates A$\beta$ fibril formation, and maintains A$\beta$ fibril stability, *J. Neurochem. 69*, 2452−2465.
11. Snow, A. D., Mar, H., Nochlin, D., Kimata, K., Kato, M., Suzuki, S., Hassell, J., and Wight, T. N. (1988) The presence of heparan sulfate proteoglycans in the neuritic plaques and congophilic angiopathy in Alzheimer's disease, *Am. J. Pathol. 133*, 456−463.
12. Webster, S., Glabe, C., and Rogers, J. (1995) Multivalent binding of complement protein C1Q to the amyloid $\beta$-peptide (A$\beta$) promotes the nucleation phase of A$\beta$ aggregation, *Biochem. Biophys. Res. Commun. 217*, 869−875.
13. Namba, Y., Tomonaga, M., Kawasaki, H., Otomo, E., and Ikeda, K. (1991) Apolipoprotein E immunoreactivity in cerebral amyloid deposits and neurofibrillary tangles in Alzheimer's disease and kuru plaque amyloid in Creutzfeldt-Jakob disease, *Brain Res. 541*, 163−166.
14. Gomez-Isla, T., Hollister, R., West, H., Mui, S., Growdon, J. H., Petersen, R. C., Parisi, J. E., and Hyman, B. T. (1997) Neuronal loss correlates with but exceeds neurofibrillary tangles in Alzheimer's disease, *Ann. Neurol. 41*, 17−24.
15. Raber, J., Huang, Y., and Ashford, J. W. (2004) ApoE genotype accounts for the vast majority of AD risk and AD pathology, *Neurobiol. Aging 25*, 641−650.
16. Palu, E., and Liesi, P. (2002) Differential distribution of laminins in Alzheimer disease and normal human brain tissue, *J. Neurosci. Res. 69*, 243−256.
17. Holtzman, D. M. (2004) In vivo effects of ApoE and clusterin on amyloid-$\beta$ metabolism and neuropathology, *J. Mol. Neurosci. 23*, 247−254.
18. Hashimoto, T., Wakabayashi, T., Watanabe, A., Kowa, H., Hosoda, R., Nakamura, A., Kanazawa, I., Arai, T., Takio, K., Mann, D. M., and Iwatsubo, T. (2002) CLAC: A novel Alzheimer amyloid plaque component derived from a transmembrane precursor, CLAC-P/collagen type XXV, *EMBO J. 21*, 1524−1534.
19. Schmidt, M. L., Saido, T. C., Lee, V. M., and Trojanowski, J. Q. (1999) Spatial relationship of AMY protein deposits and different species of A$\beta$ peptides in amyloid plaques of the Alzheimer disease brain, *J. Neuropathol. Exp. Neurol. 58*, 1227−1233.
20. Lemere, C. A., Grenfell, T. J., and Selkoe, D. J. (1999) The AMY antigen co-occurs with A$\beta$ and follows its deposition in the amyloid plaques of Alzheimer's disease and Down syndrome, *Am. J. Pathol. 155*, 29−37.
21. Söderberg, L., Zhukareva, V., Bogdanovic, N., Hashimoto, T., Winblad, B., Iwatsubo, T., Lee, V. M., Trojanowski, J. Q., and Näslund, J. (2003) Molecular identification of AMY, an Alzheimer disease amyloid-associated protein, *J. Neuropathol. Exp. Neurol. 62*, 1108−1117.
22. Franzke, C.-W., Bruckner, P., and Bruckner-Tuderman, L. (2005) Collagenous transmembrane proteins: Recent insights into biology and pathology, *J. Biol. Chem. 280*, 4005−4008.
23. Kowa, H., Sakakura, T., Matsuura, Y., Wakabayashi, T., Mann, D. M., Duff, K., Tsuji, S., Hashimoto, T., and Iwatsubo, T. (2004) Mostly separate distributions of CLAC- versus A$\beta$40- or thioflavin S-reactivities in senile plaques reveal two distinct subpopulations of $\beta$-amyloid deposits, *Am. J. Pathol. 165*, 273−281.
24. Osada, Y., Hashimoto, T., Nishimura, A., Matsuo, Y., Wakabayashi, T., and Iwatsubo, T. (2005) CLAC binds to amyloid $\beta$ peptides through the positively-charged amino acid cluster within

the collagen domain 1 and inhibits formation of amyloid fibrils, *J. Biol. Chem. 280*, 8596−8605.
25. Söderberg, L., Dahlqvist, C., Kakuyama, H., Thyberg, J., Ito, A., Winblad, B., Näslund, J., and Tjernberg, L. O. (2005) Collagenous Alzheimer amyloid plaque component assembles amyloid fibrils into protease resistant aggregates, *FEBS J. 272*, 2231−2236.
26. Aguilar, M. I., and Small, D. H. (2005) Surface plasmon resonance for the analysis of $\beta$-amyloid interactions and fibril formation in Alzheimer's disease research, *Neurotoxic. Res. 7*, 17−27.
27. Söderberg, L., Kakuyama, H., Moller, A., Ito, A., Winblad, B., Tjernberg, L. O., and Näslund, J. (2005) Characterization of the Alzheimer's Disease-associated CLAC protein and identification of an amyloid $\beta$-peptide-binding site, *J. Biol. Chem. 280*, 1007−1015.
28. Webster, S., Bonnell, B., and Rogers, J. (1997) Charge-based binding of complement component C1q to the Alzheimer amyloid $\beta$-peptide, *Am. J. Pathol. 150*, 1531−1536.
29. Tjernberg, L. O., Näslund, J., Lindqvist, F., Johansson, J., Karlström, A. R., Thyberg, J., Terenius, L., and Nordstedt, C. (1996) Arrest of $\beta$-amyloid fibril formation by a pentapeptide ligand, *J. Biol. Chem. 271*, 8545−8548.
30. Tjernberg, L. O., Callaway, D. J., Tjernberg, A., Hahne, S., Lilliehöök, C., Terenius, L., Thyberg, J., and Nordstedt, C. (1999) A molecular model of Alzheimer amyloid $\beta$-peptide fibril formation, *J. Biol. Chem. 274*, 12619−12625.
31. Tjernberg, L. O., Tjernberg, A., Bark, N., Shi, Y., Ruzsicska, B. P., Bu, Z., Thyberg, J., and Callaway, D. J. (2002) Assembling amyloid fibrils from designed structures containing a significant amyloid $\beta$-peptide, *Biochem. J. 366*, 343−351.
32. Cannon, M. J., Williams, A. D., Wetzel, R., and Myszka, D. G. (2004) Kinetic analysis of $\beta$-amyloid fibril elongation, *Anal. Biochem. 328*, 67−75.
33. Hasegawa, K., Ono, K., Yamada, M., and Naiki, H. (2002) Kinetic modeling and determination of reaction constants of Alzheimer's $\beta$-amyloid fibril extension and dissociation using surface plasmon resonance, *Biochemistry 41*, 13489−1398.
34. Shuvaev, V. V., and Siest, G. (1996) Interaction between human amphipathic apolipoproteins and amyloid $\beta$-peptide: Surface plasmon resonance studies, *FEBS Lett. 383*, 9−12.
35. Wood, S. J., Wetzel, R., Martin, J. D., and Hurle, M. R. (1995) Prolines and amyloidogenicity in fragments of the Alzheimer's peptide $\beta$/A4, *Biochemistry 34*, 724−730.
36. Wogulis, M., Wright, S., Cunningham, D., Chilcote, T., Powell, K., and Rydel, R. E. (2005) Nucleation-dependent polymerization is an essential component of amyloid-mediated neuronal cell death, *J. Neurosci. 25*, 1071−1080.

BI051263E